

**THE INTERNAL TIDAL BORE  
AT THE HEAD OF THE MONTEREY  
SUBMARINE CANYON:**

**2/3 FEBURARY 2003**

**LEUT Kristen Watts, RAN  
OC 3570  
Winter 2003**

## **1. INTRODUCTION**

A group of NPS students studying Operational Oceanography, conducted a research cruise onboard R/V Pt Sur from 27 January to 3 February 2003. Many different forms of atmospheric and oceanographic data were collected from numerous coastal stations in Monterey Bay and south, to San Luis Obispo. This report focuses on the analysis of data that was collected in the vicinity of the head of the Monterey Canyon, on 2-3 February 2003, on Leg II of this cruise. This data includes: a 25-hour time series of conductivity, temperature and depth (CTD) profiles; Acoustic Doppler Current Profiler (ADCP) measurements; and, data collected from two shallow-water Aquadopp current meter moorings.

## **2. PURPOSE**

Many studies have been previously conducted in the Monterey Canyon with the hope of describing the internal wave pattern and the internal tidal bores, which are evident at the head of the canyon. A bore is an unsteady flow, often caused by tidal forcing and can be equated to a moving hydraulic jump.<sup>1</sup> This phenomenon is clearly evident when propagating along the surface of a river, in the form of a breaking wave. Internal tidal bores are not so easy to observe, as they cannot be physically seen. As a result, their onset must be determined through analysis and comparison of various types of datasets.

A surface tidal bore occurs in some specific rivers, usually during exceptionally high tides. For this type of bore to form, the river exhibits certain characteristics; the banks form a converging funnel shape, the river bed gently rises, and the river is of considerable length.<sup>2</sup> Analogous to the surface bore, is the internal tidal bore, which can exist in areas where a submarine canyon forms a converging funnel shape, combined with a gently rising sea floor, preferably over a considerable distance. This type of topography causes an internal wave to become highly non-linear and steepen at its face, thus forming a bore.<sup>3</sup> The Monterey Canyon exhibits these particular topographical characteristics and is therefore an area of interest for the study of this phenomenon.<sup>4</sup>

The purpose of this report is to examine data collected from a 25-hour CTD time series and the ship's ADCP, as well as moored current meters, to observe the processes operating at the head of the canyon. Due to time constraints, this paper is limited to a broad analysis of the retrieved data with a view to explaining some of the results, which show evidence of the passage of an internal tidal bore.

### **3. TOPOGRAPHY OF THE MONTEREY BAY CANYON**

Figure 1 shows the bathymetry of the Monterey Canyon with the CTD station and current meter mooring locations marked. The canyon head lies within 100 m of Moss Landing. From here, the submarine canyon then meanders offshore, roughly across the centre of Monterey Bay, in a generally cross-shore direction (080-260). Over a distance

of 20 km, the canyon floor slopes from 1000 m at the mouth of the bay, to approximately 100 m at its head. The canyon also becomes narrower inshore.<sup>5</sup>

#### 4. DATA COLLECTION

**CTD** – Using the ship's Seabird CTD, a 25-hour time series of CTD casts was conducted in the vicinity of the head of the Monterey Canyon, centred on position  $36^{\circ}47.909\text{N}$ ,  $121^{\circ}49.072\text{W}$ . Data collection began at 0200 PST on 02 February and ended at 0300 PST on 03 February 2003. Thirty CTD casts were conducted with measurements being recorded every metre, to a minimum depth of 130 m, which corresponds to a near-bottom measurement. In order to prevent accidental damage to the CTD equipment, a safety margin of approximately 20 m between the CTD and the recorded bottom was used.

**ADCP** – Throughout the CTD time series, measurements were also collected from the ship's onboard ADCP. The RD Instruments ADCP uses the Doppler affect to measure current velocity profiles. A short pulse of sound is transmitted at 150 kHz and the ADCP measures the change in pitch or frequency of the returning echo. The sound reflects off particles suspended in the water. These particles can be considered to be moving at the same speed as the water and hence, the ADCP ultimately measures the water velocity.<sup>6</sup> Figure 2 shows the positions from which ADCP data were collected. Any data that was recorded from a position greater than 1 km away from the CTD station was discarded, for the purposes of this analysis.

**MOORED CURRENT METERS** – Two Nortek Aquadopp Current Meters were mounted in fibreglass tripods and moored in shallow water, either side of the head of the Monterey Canyon. These instruments were operational from 27 January to 3 February 2003. Instrument number 636 was moored in position  $36^{\circ} 48.80\text{N}$ ,  $121^{\circ} 48.08\text{W}$  in 16 m of water, on the northern side of the canyon. Instrument number 669 was moored in position  $36^{\circ} 47.72\text{N}$ ,  $121^{\circ} 48.28\text{W}$  in 17 m of water, on the southern side of the canyon. The Aquadopp uses the Doppler effect to measure current velocity and transmits a short pulse of sound, at a frequency of 2 MHz. The Aquadopp also has a pressure sensor, which can be used to infer changes in water level.<sup>7</sup>

Data collected from these two instruments was used to create vector plots of the currents at the top of the water column as well as ancillary data plots, such as pressure and temperature differences. These two current meters have previously been compared against one another, for calibration purposes. It was discovered that the northern instrument only has an effective range to about 8 metres from the bottom. As a result, this data is rather limited in its use and data from the southern instrument has mainly been used, for the purposes of this analysis.

#### **4. DATA ANALYSIS AND INTERPRETATION**

Figure 3 shows the temperature and salinity time series constructed from the CTD data, collected at the head of the canyon. From the displacement of the isotherms and isohalines, it is clear to see that there is an internal wave propagating through the water

column. The wave signal is more pronounced with depth, as there is a larger displacement of the contours near the bottom, compared with that of the surface. There does seem to be some phase lag however between the signal at the top and the bottom of the water column, when looking at the wave troughs. In both cases, a line through the trough appears to slope slightly with height. The trough is evident at the surface before it appears at the bottom, with a time lag of the order 1-2 hours. When looking at the wave crests however, or the maximum upward displacement of the contours, the phase lag is minimal and the crest appears almost vertical through the water column. This observation of troughs sloping through the water column but crests being vertical, leads to the conclusion that this internal wave is in fact non-linear.

Figure 4a shows the pressure variation as recorded by the southern Aquadopp. This data can be equated to the variation in sea level and the tidal cycle. Sea level data from the Monterey tide gauge (9413450) was also obtained and examined. The plot produced was very similar to the Aquadopp plot and showed the same pattern and height variations in sea level. The Monterey tide gauge data only has a resolution of 6 minutes so any small variations between the two data sets are negligible. As a result, the plot obtained from the Aquadopp profiler data, was used for comparisons between the mean sea level and observed changes in other quantities. From this figure, it is easy to see that Monterey Bay exhibited a mixed semi-diurnal tidal cycle during this time period. A high water of 1.8 m at 1011 PST and a low water of  $-0.2$  m at 1742 PST can be attributed to the diurnal constituent of the tide whilst a lower high water of 1.3 m at 0024 PST and a

higher low water of 0.7 m at 0412 PST, can be attributed to the semi-diurnal cycle of the tide.

A comparison between the temperature as measured by the southern Aquadopp and vertically averaged temperature, as measured from the CTD, is shown in figure 4b. Both data sets show a similar pattern with the Aquadopp showing some small variations, which are not evident in the CTD data, as they would be removed when vertically averaging. From figures 3 and 4, it appears that the crest of the internal wave, or the minimum in average temperature and salinity, occurs during the ebb tide, approximately halfway between the highest barotropic high water and the lowest barotropic low water.

Figure 5 shows the current component profiles in the top 16m of the water column as recorded by the southern Aquadopp. The current data was divided into the normal  $u$  (east/west) and  $v$  (north/south) components, where a north component equates to a flow to the north and similarly for the other components. Due to the meandering of the canyon, this does not necessarily equate to along- and across-canyon flow but at the canyon head, the  $u$  component is nearly along-canyon. Here, the flow shows more variability in the north/south direction than the east/west direction. A strong northward flow of about 40 cm/s is evident with the occurrence of the beginning of the tidal floods and a less strong southward flow of around 20cm/s is evident with the beginning of the ebb flow. This data only represents measurements of the very top of the water column, and shows that tidal forcing essentially drives the surface current.

The current component profiles for the northern Aquadopp, are shown in figure 6. A comparison between the two Aquadopp measurements shows that the variability in current speed and direction, for the northern mooring, is much less than the values for the southern mooring, even though the most variation still occurs in the north/south, or alongshore, direction. The northern instrument shows a relatively weak current flow, which rarely exceeds 20 cm/s and is generally in the northeastward direction. The onset of the northward flow at the northern instrument lags the onset at the southern instrument by approximately 2-3 hours. The cause of this considerable disparity between currents on the northern and southern rim of the canyon is not clear, but could be due to significant differences in the canyon topography at each station, as well as the exact location of each mooring, in relation to the rim of the canyon.

Figure 7 shows a vector plot of the southern Aquadopp currents, measured at 1.2 m from the bottom. This equates to the deepest depth measured by the instrument and a depth in the water column of about 15 m. A plot of pressure is also included, in order to compare the observed changes in relative surface layer currents with the tidal cycle. A strong northward current of around 40 cm/s occurs during the diurnal flood tide and the current rotates to the south during the ebb. For the semi-diurnal tidal component, however, the northward current begins at the end of the ebb, just before the low water. The flood tide is characterised by a northward component, initially, which becomes southward about 2-3 hours after the low water. The currents associated with the diurnal cycle are around 10 cm/s greater than those associated with the semi-diurnal cycle.



The velocity profile constructed from the ADCP measurements is shown in figure 8. This data shows more variability in the east/west direction than the Aquadopp, particularly at the canyon bottom. Westward, or offshore flows, at the bottom, are associated with the rising tide whilst eastward, or onshore flows, are associated with the falling tide, but this is only for the diurnal constituent, or the highest high water. For the semi-diurnal tidal cycle, the offshore flow occurs in conjunction with the low water, whilst the onshore flow occurs with the rising tide. The magnitude of the offshore current is of the order 5-10 cm/s larger than the onshore flow. From these observations, there appears to be a distinct difference in the behaviour of the water column with respect to phase of the diurnal and semi-diurnal surface tidal components. As a result, it is expected that some other process is acting as the forcing mechanism for the internal currents, rather than just the barotropic tidal forcing.

Vertically averaged ADCP current velocity for the entire time series is shown in figure 9. The most obvious feature in this data is the distinct reversal of the average current over the water column, which occurs at around 1400 PST. The averaged flow shifts from relatively strong flow to the northeast to a similar magnitude flow towards the southwest. When compared to the canyon topography in figure 1, this equates to an up-canyon flow abruptly shifting to a down-canyon flow. The strongest currents throughout the water column occur just before 1800 PST, however the magnitude of this flow appears somewhat anomalous when compared to the rest of the time series.

This distinct current reversal, as shown in the ADCP measurements, was compared with the previous figures and it was found that it coincided with the crest of the internal wave or the maximum upward displacement of the contours of temperature and salinity. When compared to figure 4b, the timing occurs at the point where the temperature recorded by the Aquadopp, as well as the vertically averaged temperature from the CTD, reaches a minimum. It is difficult to determine whether a similar pattern will occur at each wave ridge due to the fact that the first ridge occurs before the beginning of the time series and the third ridge occurs right at the end of the period.

Figure 10 shows the currents as measured by the southern Aquadopp at four different bins at the top of the water column. As the instrument was moored in 17 m of water, this figure represents depths from the surface to 15 m. The strongest currents exist at about 0600 PST, in conjunction with the beginning of the tidal flood and again at 1700 PST, near the time of the lowest low water. At around 1400 PST, there is a distinct reversal of direction as well as an increase in velocity, which coincides with the timing of the current reversal as discovered in the averaged ADCP data. The reversals in current direction as measured by the Aquadopp at the surface, coincide almost exactly with the shifts in current direction which are evident at the bottom in the ADCP velocity profiles, but the components are predominantly in the alongshore direction as opposed to the cross-shore direction.

## **5. RESULTS/DISCUSSION**

According to the literature, the arrival of an internal tidal bore is characterised by wave steepening, a sharp drop in temperature and salinity over the water column, as well as a significant increase in upslope current velocity at the bottom.<sup>8</sup> From analysis of the results presented here, it is therefore consistent with the passing of a bore at around 1400 PST on 2 Feb 2003. At this time, there is a sharp drop in temperature and salinity, characterised by the maximum upward displacement of the isotherms and isohalines. Occurring at the same time is an abrupt reversal in the vertically averaged ADCP velocity data, from the north-eastward (up-canyon) direction to south-westward (down-canyon) direction.

This change in current direction is also clearly evident in the east/west ADCP velocity profiles. At around 1400 PST, the flow at the bottom changes from a relatively weak north-eastward flow of 0-5 cm/s, to a south-westward flow, which increases to a maximum speed of about 25 cm/s. The maximum velocity observed at the bottom does however lag the abrupt current reversal by about 2-3 hours.

When compared to the tidal data, the bore occurs during the ebb, approximately mid way between the highest barotropic high tide, and the lowest barotropic low tide. According to the literature, the passing of the internal bore should result in a strong upcanyon surge and the pumping of cooler, more saline waters from the canyon onto the adjacent continental shelf.<sup>9</sup> This process would be expected to occur with strong onshore currents at the bottom. The displacement of this water will cause a hydrostatic imbalance between the cool, saline water inshore and the warm salty water offshore.<sup>10</sup> At this point,

the currents will reverse due to density and the cold water will once again be pushed offshore.

From the analysed data, it can be seen that the onset of the bore occurs at the change from onshore to offshore flow at the bottom, rather than at the time of maximum velocity, as suggested in the literature. When looking into this apparent disparity between the bores as described by literature and the processes operating here, it was discovered that this observed bore more closely exhibits a standing wave pattern rather than a propagating wave. Figure 11 is a summary of the previous figures and was constructed in order to view a comparison between the timing of the barotropic tide, the internal wave propagation and the variation in the surface and bottom currents. A plot of negative vertically average temperature from the CTD data was used to simulate the up and downward displacement of the thermocline and the subsequent internal wave pattern. Only the east/west velocity component for the vertically averaged ADCP data is shown, as this was the direction that exhibited the greatest variability. Similarly, only the north/south component has been plotted for both of the Aquadopp current meters.

The red vertical line equates to the position of the observed internal tidal bore. It is clear to see that this bore occurred halfway between the high and low waters, at the time of maximum upward displacement of the thermocline and in conjunction with the change of average velocity from eastward to westward.

From these observations, it is considered that the bore was in fact a standing internal tidal bore. A standing wave is formed by the constructive interference of two waves, which travel in opposite directions in a medium.<sup>11</sup> A wave is reflected from a barrier and there is a  $180^0$  change in the phase of the reflected wave. A schematic model of a standing wave is shown in figure 12.<sup>12</sup> In the observed situation, it is considered that the head of the canyon acts like a barrier to reflect the waves. The bore occurs at the time of zero east/west velocity through the water column. From a standing wave model, this means that the movement of water in the water column at this point would be primarily up and down. It is therefore considered that the bore acts to pump water upward and downward at the canyon head.

When looking at the Aquadopp velocities, it is evident that the bore occurred at the change in alongshore current directions for both instruments. However, at the southern instrument, the change was from southward to northward velocity but was opposite for the northern instrument which changed from a northward to a southward flow. This then leads to the assumption that the bore is actually sucking water down into the canyon because at the time of its passage, the northern Aquadopp exhibits a weak southward velocity while the southern instrument exhibits a strong northward velocity.

From observations of the periodicity of the observed data and the precursors to the appearance of a bore, it seems plausible to assume that a bore occurred just prior to the start of data collection and is in the process of occurring at the end of the period. A longer time series and study of all the relevant observations would be required to confirm

the periodicity or frequency of the passage of internal tidal bores in this area. This study only represents measurements at the head of the Monterey Canyon and in order to observe the propagation of the bore along the entire canyon length, and possibly the processes operating for bore formation; other moorings would need to be placed at intervals along the canyon axis.

## **6. CONCLUSION**

From observations of data it is evident that the mechanisms for internal waves and standing tidal bores were operating during the 25 hours in which data was collected at the head of the Monterey Canyon. A complete understanding of these processes cannot be obtained though this short, limited study but would need more thorough research and a much longer time series of data. The results obtained through this analysis provide only a very brief glimpse of the wide and varied processes operating throughout the intricate and fascinating Monterey Canyon.

## **7. REFERENCES**

1. G.F. Lane-Serff, D.R. Munday and M.D. Woodward, 'Laboratory experiments of internal bores in non-rotating and rotating exchange flows over sills,' The 2<sup>nd</sup> Meeting on the Physical Oceanography of Sea Straits, Villefranche, 2002.
2. Linden Software – Tidal Bores: [www.linden-software.com/tidal1.html](http://www.linden-software.com/tidal1.html)

3. S.A. Key, 'Internal Tidal Bores in the Monterey Canyon', Thesis, Naval Postgraduate School, Monterey, California, 1999.
4. E.T. Petruncio, L.K. Rosenfeld and J.D. Paduan, 'Observations of the Internal Tide in Monterey Canyon', *Journal of Physical Oceanography*, October 1998.
5. *ibid.*
6. Acoustic Doppler Current Profilers – Principles of Operation: A Practical Primer, RD Instruments, January 1, 1989.
7. Aquadopp Operations Manual, Nortek USA, San Diego, November 1, 2000.
8. J. Leichter, 'Input of nutrients to reefs in Florida Keys by upwelling,' Woods Hole Oceanographic Institution. [www.uncwil.edu/nurc/aquarios/2000/6\\_2000/expd.htm](http://www.uncwil.edu/nurc/aquarios/2000/6_2000/expd.htm)
9. J. Pineda, 'Issues in larval transport by internal tidal bores,' Woods Hole Oceanographic Institution.  
[www.whoi.edu/science/AOPE/people/tduda/isww/text/pineda/pineda.htm](http://www.whoi.edu/science/AOPE/people/tduda/isww/text/pineda/pineda.htm)
10. J.J. Leichter, S.R. Wing, S.L. Miller and M.W. Denny, 'Pulsed delivery of subthermocline water to Conch Reef (Florida Keys) by internal tidal bores,' *Limnology and Oceanography*, 41(7): 1490-1501, 1996.

12. T. Henderson, 'Standing Waves,' 2001.

[www.glenbrook.k12.il.us/gbssci/phys/Class/waves/u1014b.htm](http://www.glenbrook.k12.il.us/gbssci/phys/Class/waves/u1014b.htm).

13. *ibid.*



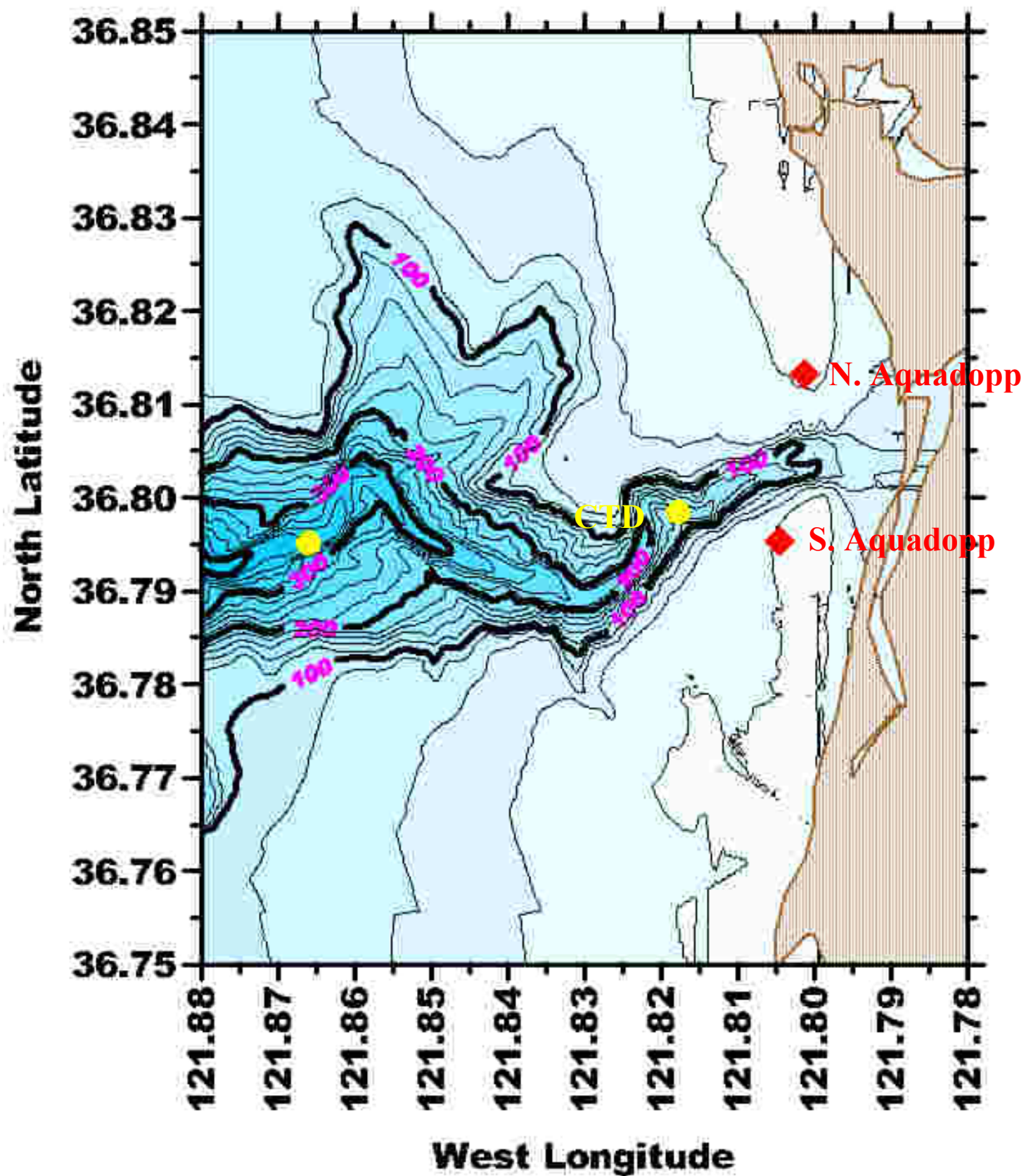
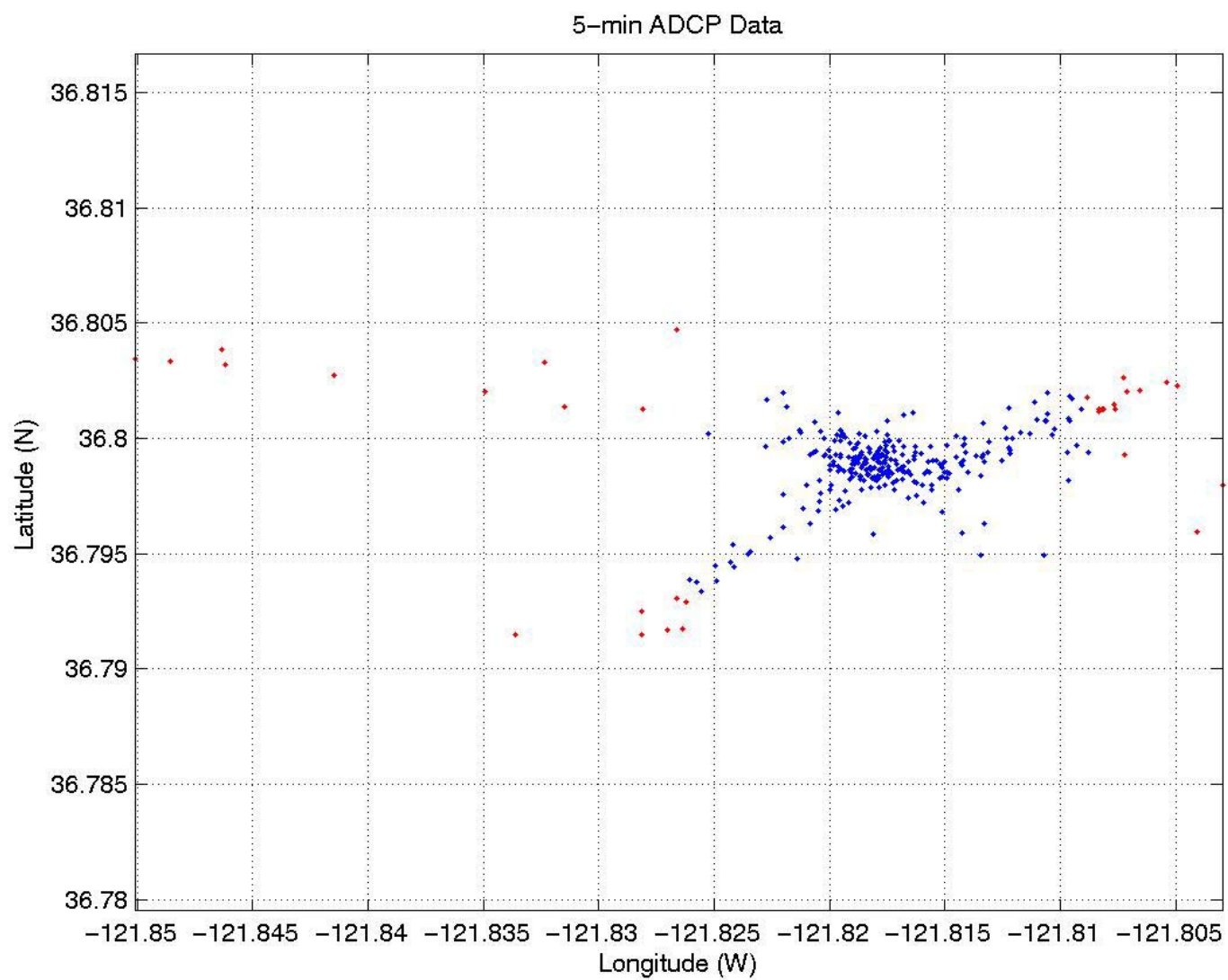


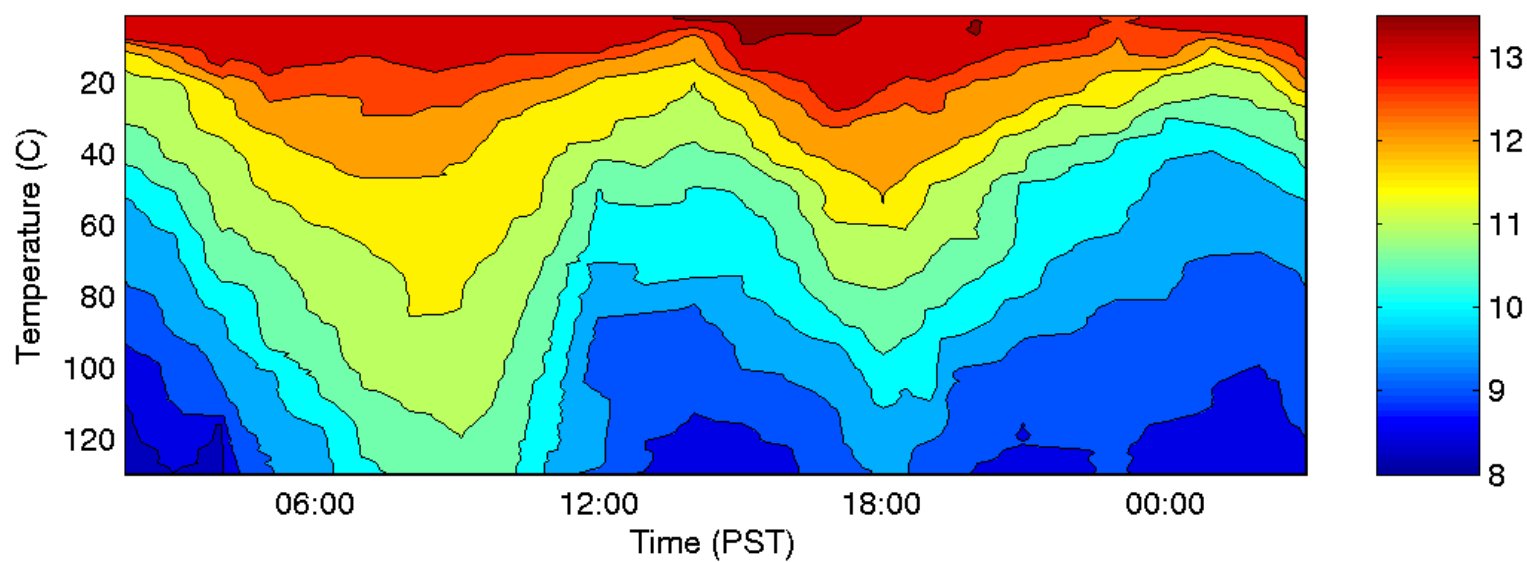
Figure 1: Bathymetry at the head of the Monterey Canyon with the CTD station and current meter moorings marked.



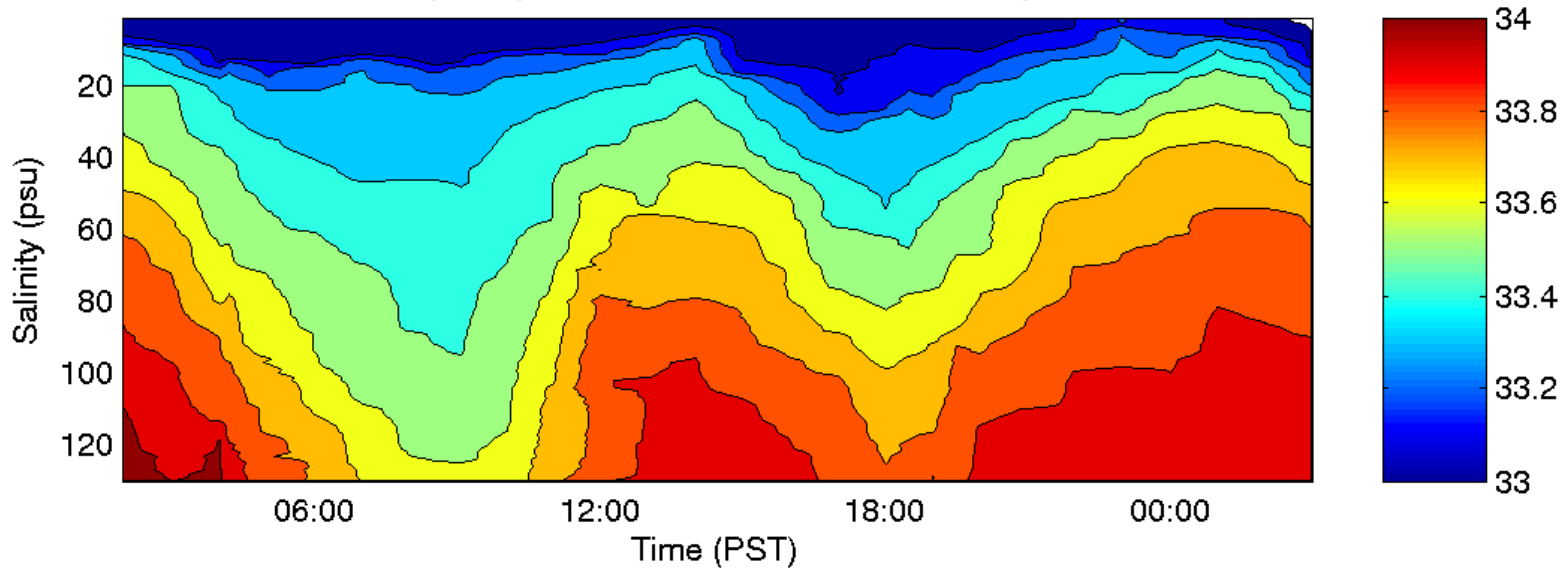
**Figure 2:** The positions from which ADCP data were collected. Red dots indicate that the position was greater than 1km away from the CTD station and this data was discarded for the purposes of this analysis.

**a.**

Monterey Canyon CTD Time Series: 2–3 February 2003

**b.**

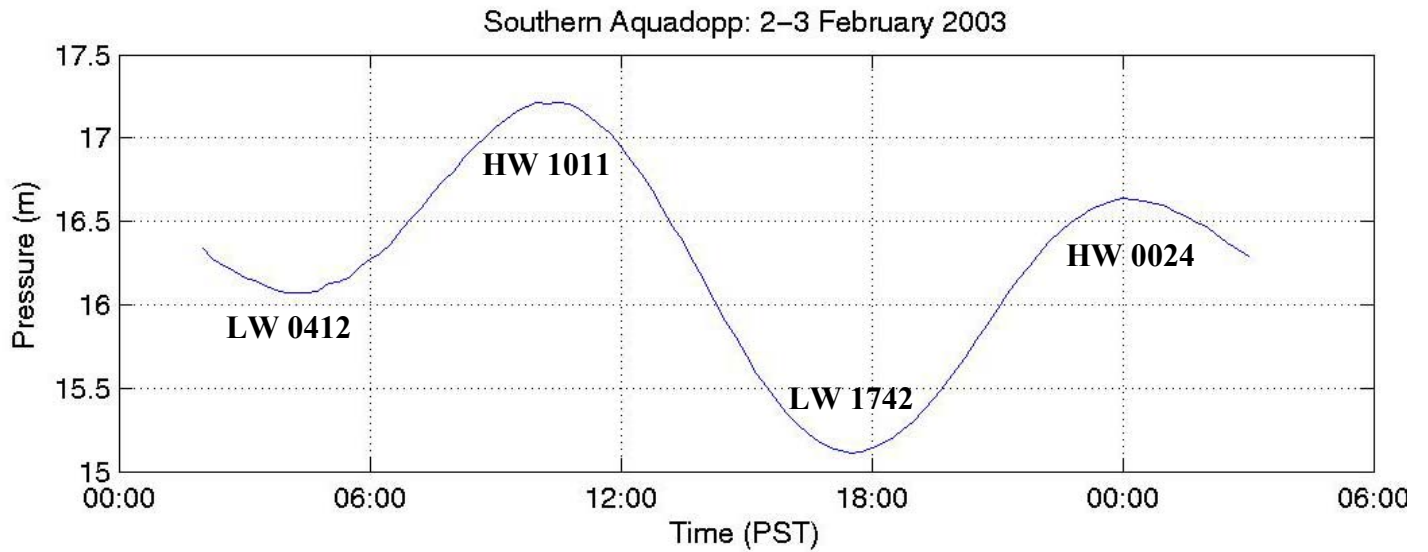
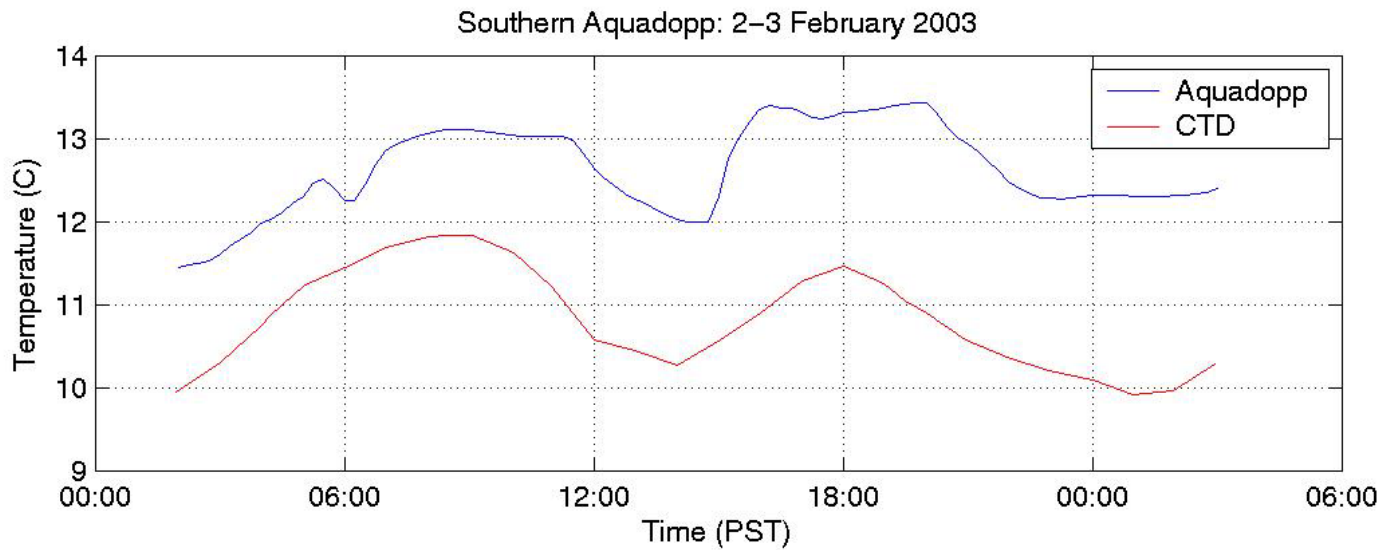
Monterey Canyon CTD Time Series: 2–3 February 2003



**Figure 3:** Time Series profiles taken from CTD measurements at the head of Monterey Canyon on 2-3 February 2003.

**a.** Temperature.

**b.** Salinity.

**a.****b.**

**Figure 4: Observations from the southern Aquadopp:**

**a.** Pressure variation with high and low waters marked. Tidal height data is from the Monterey Tide Gauge records.

**b.** Temperature recorded by the Aquadopp, compared with vertically averaged temperature recorded from the CTD time series.

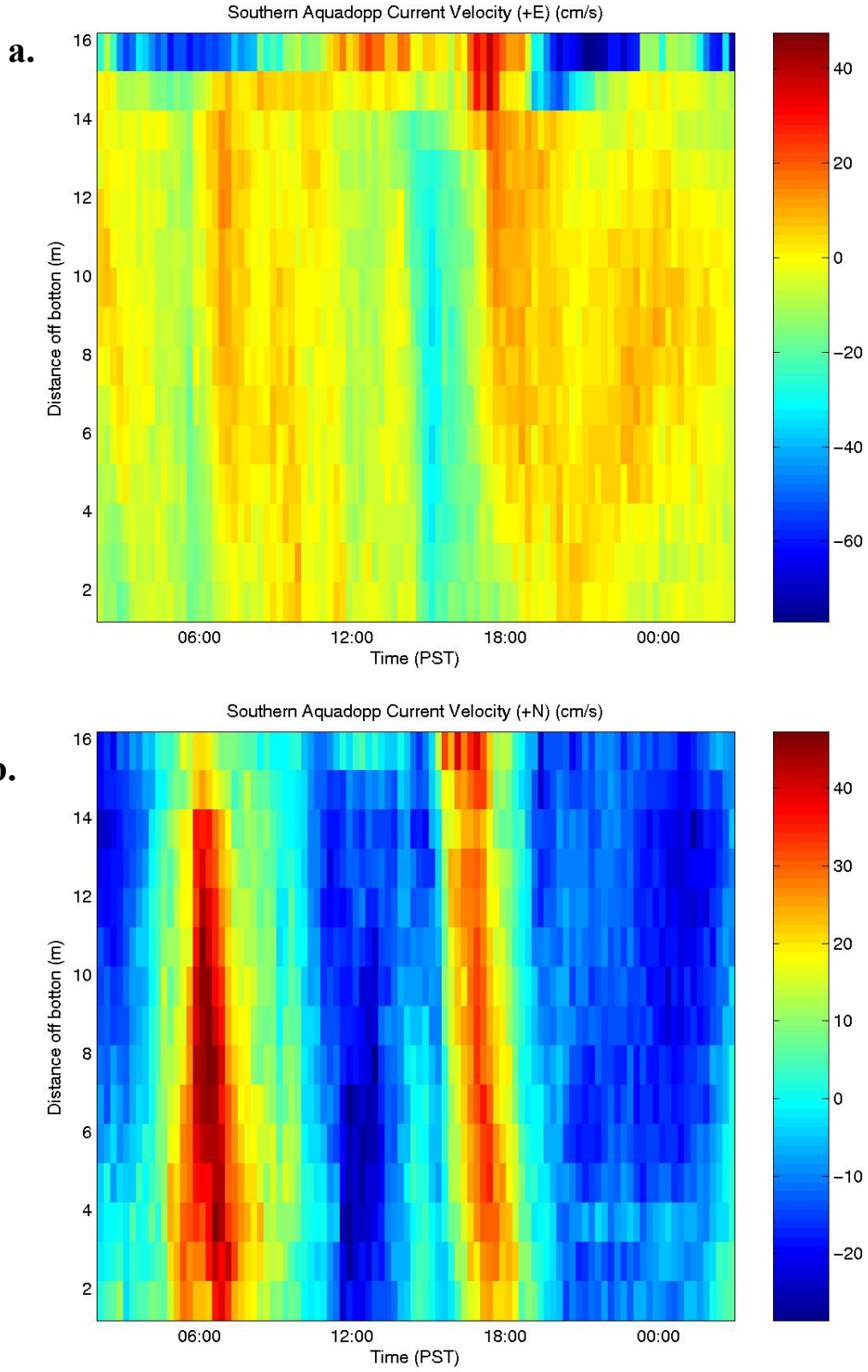


**Figure 5:** Current velocities as measured by southern Aquadopp;  
**a.** east/west component and **b.** north/south component.



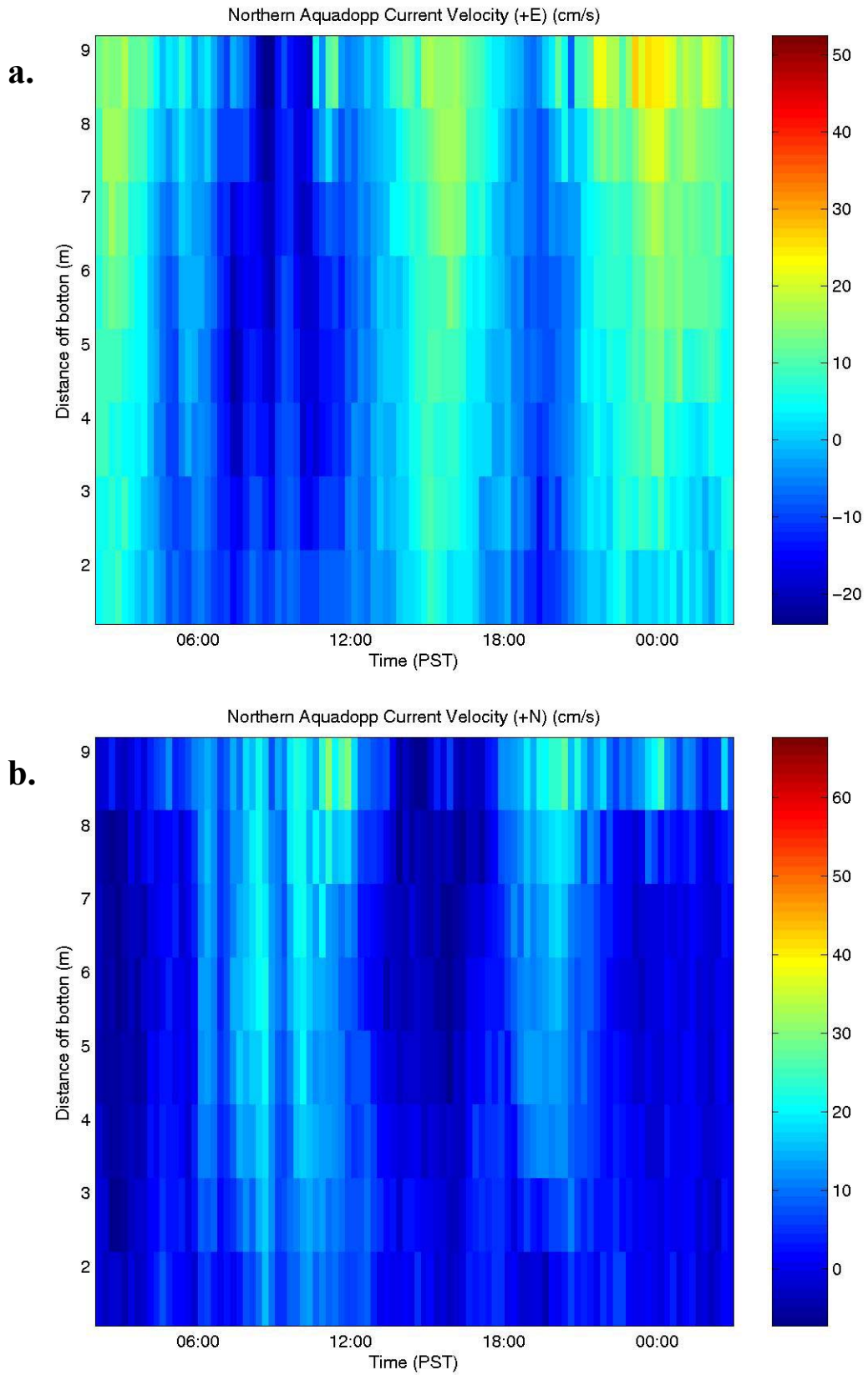
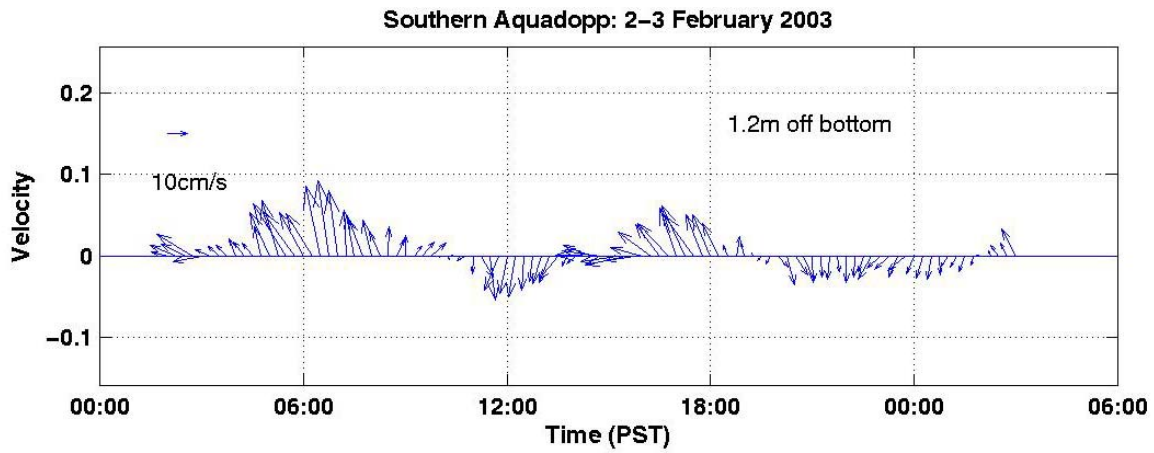
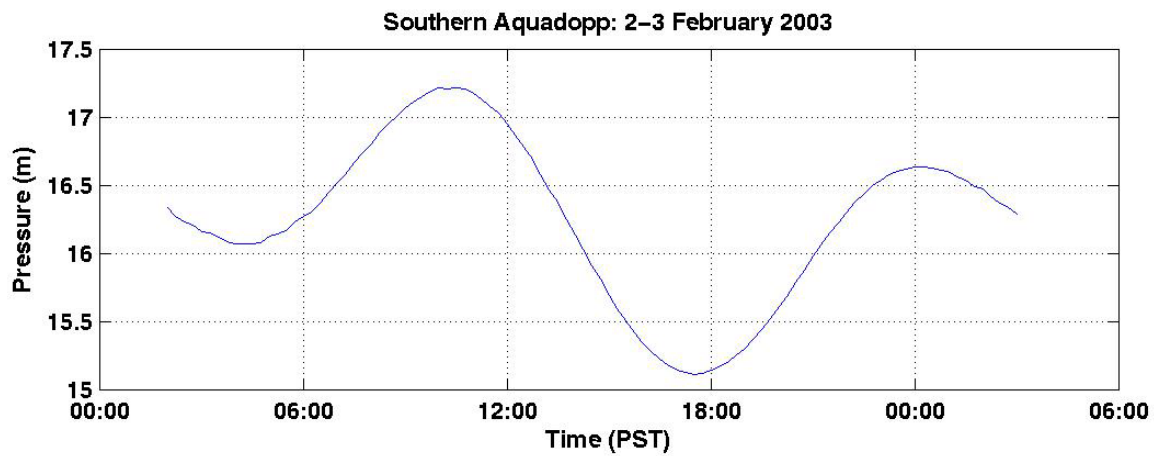


**Figure 6:** Current velocities as measured by northern Aquadopp; a. east/west component and b. north/south component.

a.



b.

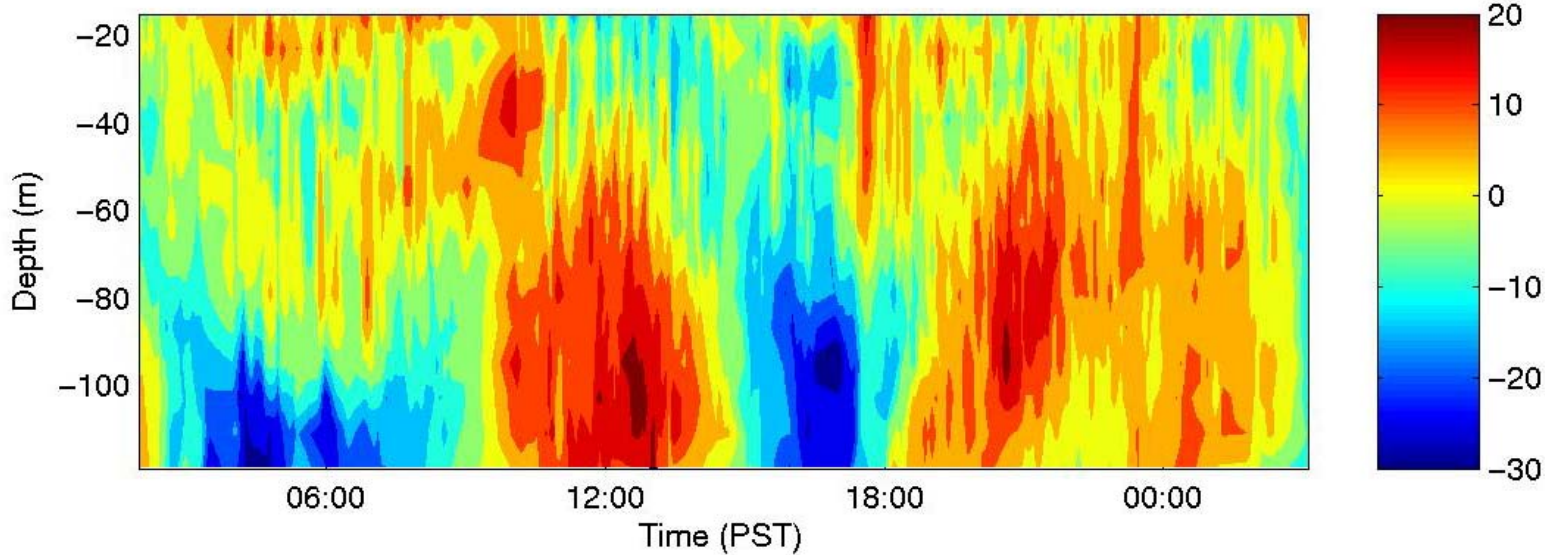


**Figure 7: Data recorded by southern Aquadopp;**

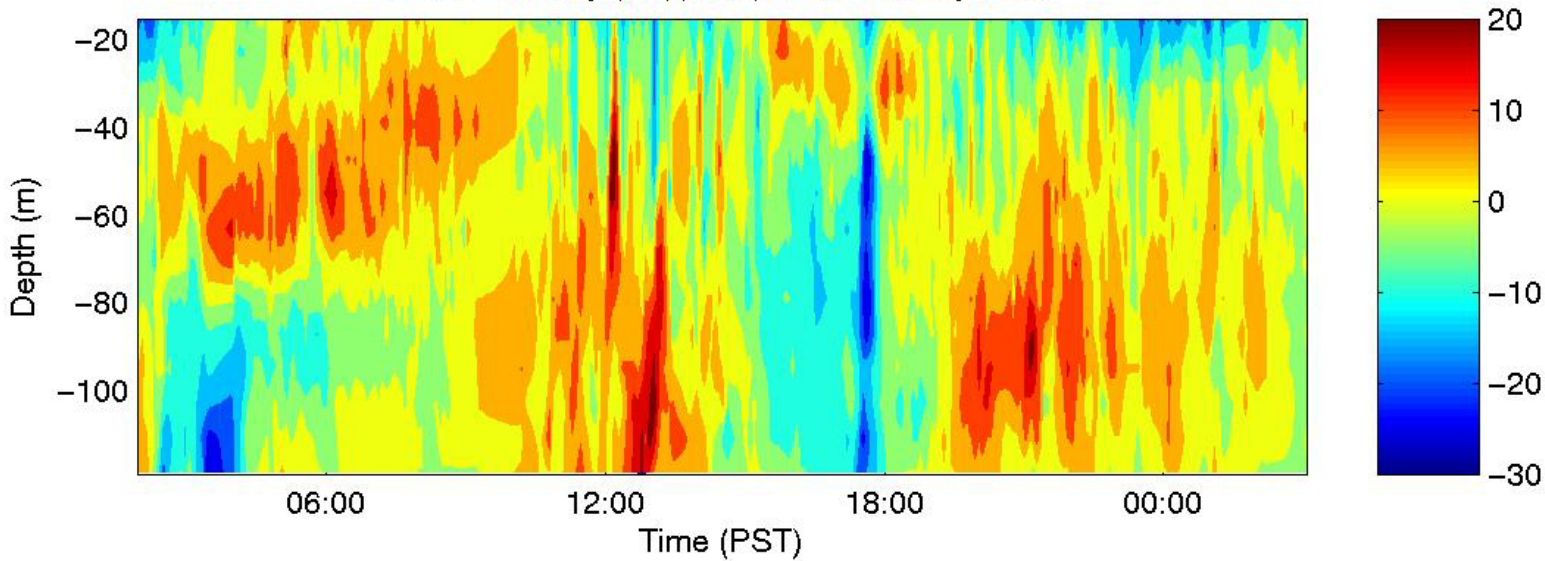
- a. Vector plot of currents measured at 1.2m from the bottom.
- b. Pressure variation.

**a.**

ADCP Velocity (+E)(cm/s): 2–3 February 2003

**b.**

ADCP Velocity (+N)(cm/s): 2–3 February 2003

**Figure 8: ADCP velocity components;****a. east/west direction****b. north/south direction.**



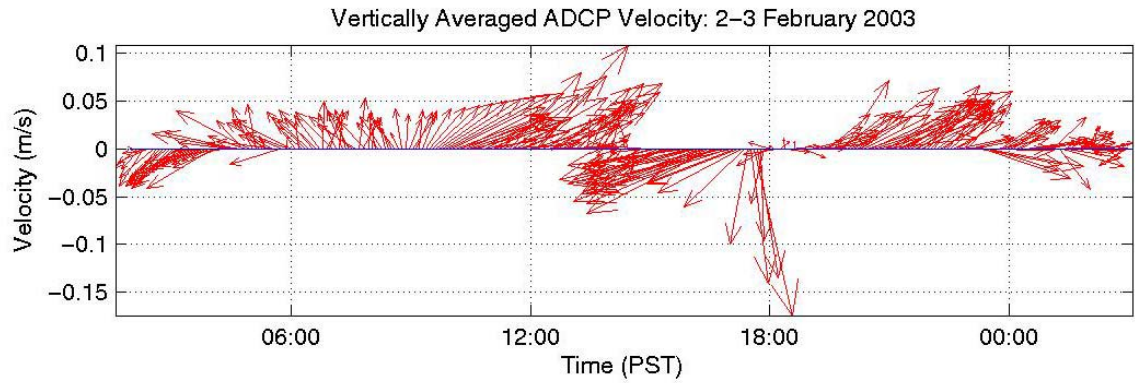


**Figure 9:** Vertically averaged ADCP current velocity time series.

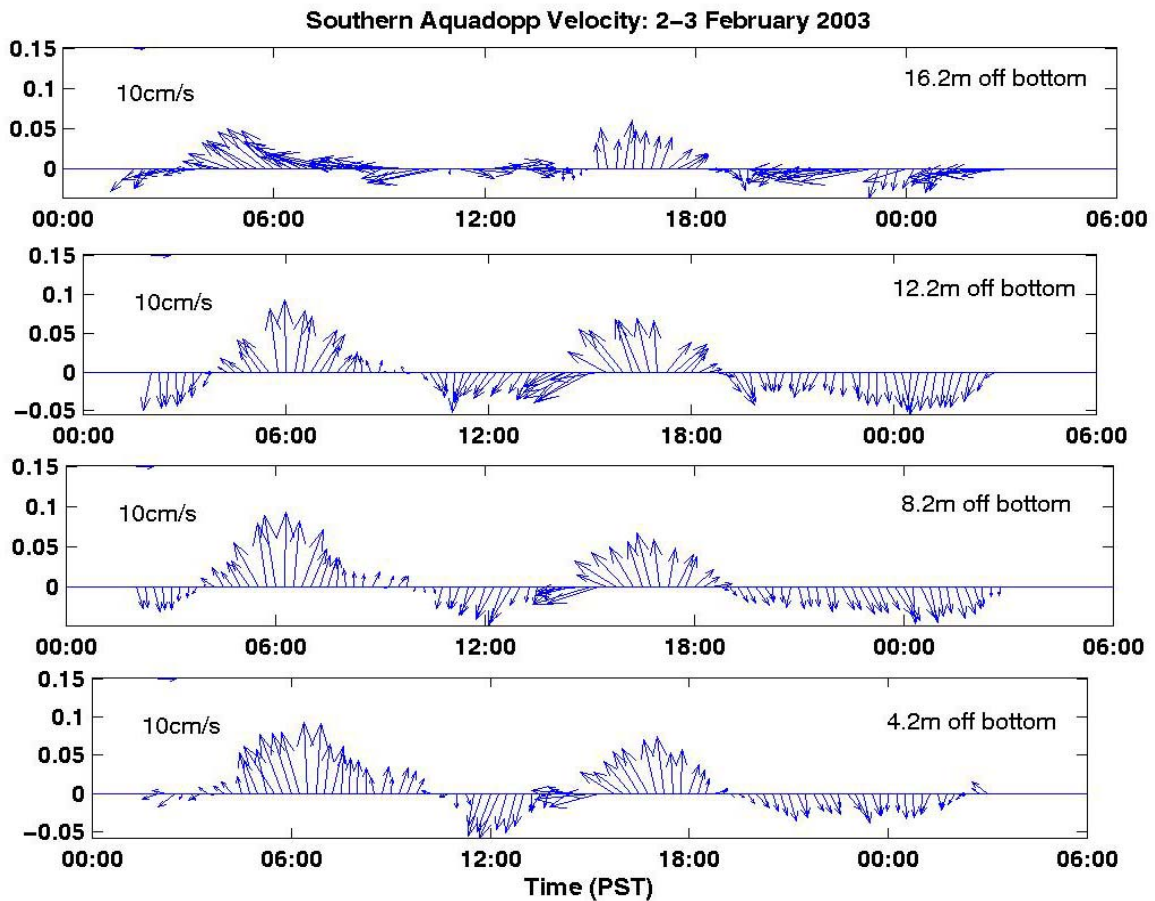


**Figure 10:** Currents measured by southern Aquadopp at four different bin intervals.

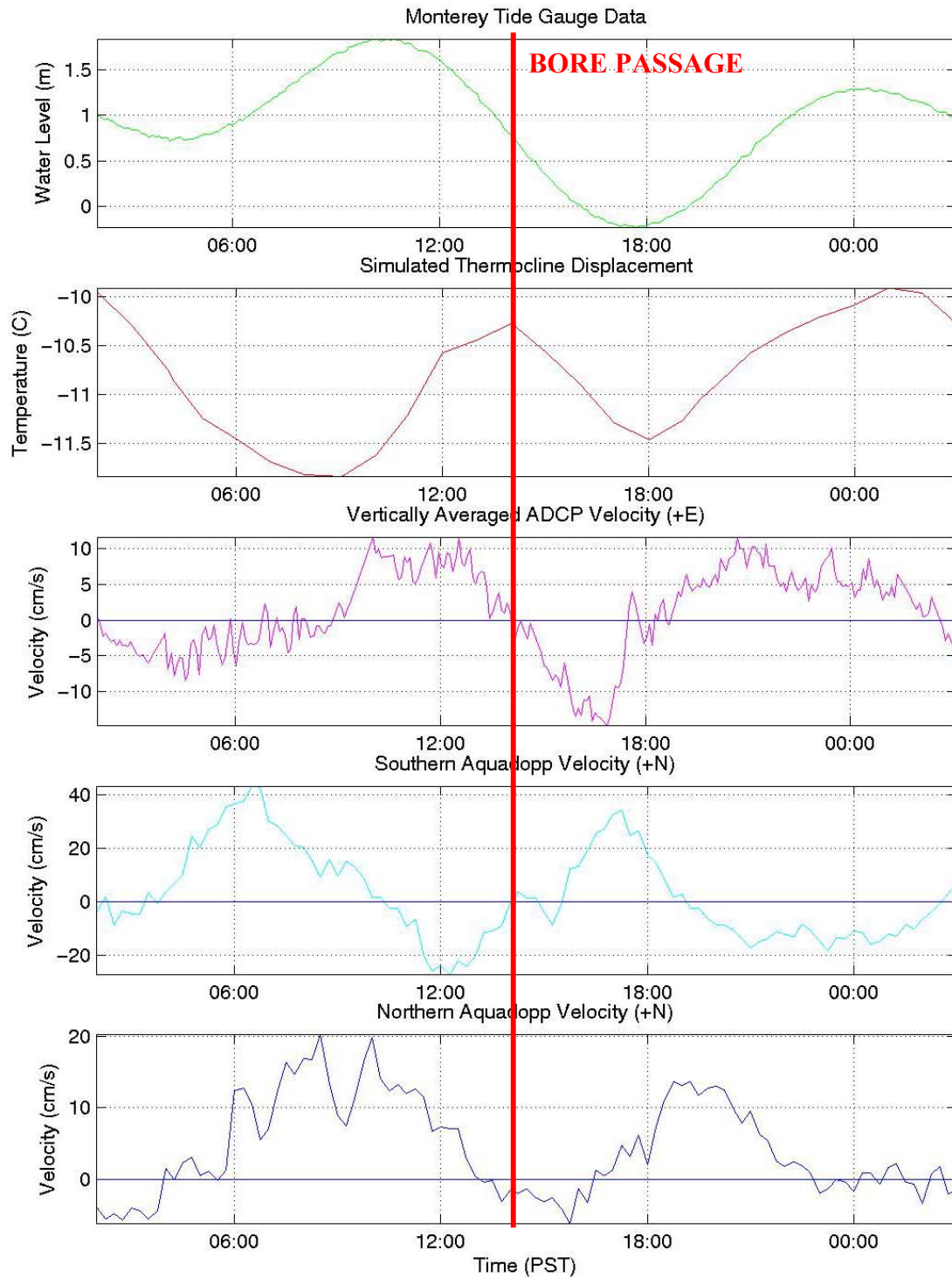


**Figure 11: Summary of previous figures with red line indicating the timing of the passage of the internal tidal bore. (North/south component represents a flow to the north/south and similarly for the east/west component)**

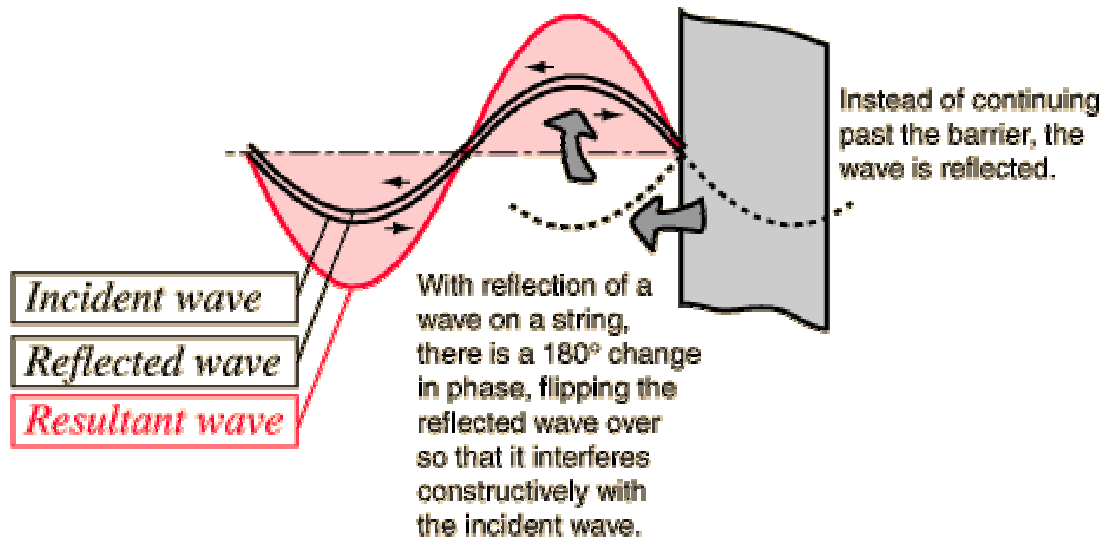


Figure 12: A schematic of a standing wave.